Inhibitive Effect of Polyacrylamide Grafted with Fenugreek Mucilage on Corrosion of Mild Steel in 0.5 M H_2SO_4 at 35°C

Varsha Srivastava, Sitashree Banerjee, M. M. Singh

Department of Applied Chemistry, Institute of Technology, Banaras Hindu University, Varanasi 221005, India

Received 21 March 2009; accepted 22 September 2009
DOI 10.1002/app.31559
Published online 10 December 2009 in Wiley InterScience (www.interscience.wiley.com).

ABSTRACT: The inhibitive effect of polyacrylamide grafted with fenugreek mucilage, a natural grade polysaccharide, on the corrosion of mild steel in 0.5*M* H_2SO_4 has been investigated by weight loss, potentiodynamic polarization and electrochemical impedance spectroscopy. An inhibition efficiency of 78% has been obtained at a concentration as low as 1 ppm and efficiency as high as 96% at 100 ppm. The polarization studies reveal that it acts as a predominantly cathodic inhibitor. The adsorption of this inhibitor on the mild steel surface obeys a Langmuir adsorption isotherm. The deposited films on the electrode surface have been analyzed by using microscopic techniques. © 2009 Wiley Periodicals, Inc. J Appl Polym Sci 116: 810–816, 2010

Key words: mild steel; Fen-*g*-PAM; corrosion inhibition; adsorption

INTRODUCTION

The corrosion inhibition of mild steel is a subject of tremendous technological importance because of the increased industrial applications of this material.[1] Acid solutions are widely used for the removal of undesirable scale and rust in many industrial processes, for examples acid cleaning of boilers, pickling of metals, and scale removal. Inhibitors are generally used during these operations to control the metal dissolution as well as the consumption of acid.[2,3] The selection of an inhibitor is governed by its economic feasibility, efficiency and side effects on the environment. Organic compounds containing nitrogen, sulphur, oxygen, heteroatoms, aromatic rings or multiple of these have been vastly used as corrosion inhibitors.[4–10] The inhibitive action of these compounds is related to the presence of one or more than one atom (site) with unshared electron pairs. Besides the number of heteroatoms, the surface area of organic molecules plays a vital role in determining their inhibition efficiency.[11] However, the application of these organic compounds has limited utility in view of higher doses of these compounds required for desired efficiency and their toxic nature. Study of metal complexes as a new class of corrosion inhibitors for different systems has been successfully accomplished and it has been invariably found that the complexation of organic base with metal ions results in increased inhibition efficiency.[12,13] More recently polymers and grafted copolymers have been evaluated for their inhibition properties on the corrosion of mild steel in acid solutions.[14–17]

Attention has been focused on the corrosion inhibiting properties of plant extracts, because plant extracts serve as incredible rich sources of naturally synthesized chemical compounds that are environmentally acceptable, inexpensive, readily available and can be extracted by simple procedures. The preparation and application of functional polymers and copolymers is one of the most important research areas in industries. Polyacrylamide (PAM) has been previously used as corrosion inhibitor for mild steel in acidic medium.[18] The incorporation of natural polysaccharides onto the backbone vinyl monomer of PAM allows the resultant copolymers to show novel functionality,[19] which possibly increases the corrosion inhibiting properties. The advantages of using fenugreek mucilage for grafting polyacrylamide lies in its occurrence in incredibly rich sources as well as its biodegradability. In the view of above, the inhibition effect of polyacrylamide grafted fenugreek mucilage on the corrosion of mild steel in 0.5*M* H_2SO_4 has been studied and the results thereof have been illustrated in the present communication.

EXPERIMENTAL

Materials

Polyacrylamide grafted fenugreek mucilage (Fen-*g*-PAM) was synthesized by grafting acrylamide onto

Correspondence to: M. M. Singh (mmsingh.apc@itbhu.ac.in).

Contract grant sponsor: UGC.

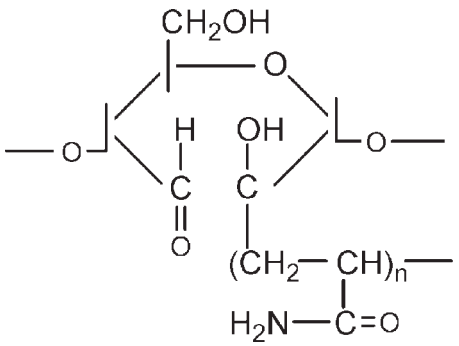

Figure 1 Structure of polyacrylamide grafted with fenugreek mucilage (Fen-*g*-PAM).

fenugreek mucilage (Fen) backbone by ceric ion initiated solution polymerization technique under nitrogen atmosphere according to Mishra et al.[19] The Fen-*g*-PAM was characterized by Fourier Transform Infrared spectroscopy (FTIR), Scanning Electron Microscopy (SEM), X-ray Diffraction (XRD), Thermo Gravimetric Analysis (TGA) and was assigned the structure as shown in Figure 1.

Analytical reagent grade H_2SO_4 was diluted with triple distilled water to obtain 0.5*M* H_2SO_4. Mild steel samples having percentage composition: C, 0.23; Mn, 0.11; Si, 0.02; P, 0.02; S, 0.02; Ni, 0.02; Cu, 0.01; Cr, 0.01; Fe, remainder, were used as test specimens.

Procedure

Gravimetric experiments were carried out in a 250 mL beaker containing 150 mL of 0.5*M* H_2SO_4 with 1–100 ppm of Fen-*g*-PAM (test solution) added to it. The steel specimens used have a rectangular form (4 × 3 × 0.1 cm^3) and were dipped into the test solution. The tests were performed for 24 h duration in an air thermostatted at 35°C. At the end of the tests, the specimens were carefully washed with water, degreased with acetone and then weighed. The experiments were repeated three times in each case and the mean value of the weight loss has been used to determine the corrosion rate. The percentage inhibition efficiency (*IE)* was calculated by using the formula[20];

$$\%IE = \frac{W^0 - W}{W^0} \times 100 \quad (1)$$

where, *W* and *W*° are the weight loss with and without the addition of polymer, respectively.

The electrochemical experiments were done using a conventional three-electrode cell assembly at 35°C. The working electrode was a mild steel sample of size (3 × 1 × 0.1 cm^3) with an exposed area of 1 cm^2 and the rest being covered with extra pure paraffin wax. The cell consisted a platinum counter electrode and a silver/silver chloride electrode as the reference electrode. The working electrode was successively polished with different grades of emery paper (320, 600, 800, 1000, 1500, and 2000), washed with water and then degreased with acetone. It was immersed in the acid solution for 30 min until a steady-state potential was reached. All tests were performed at 35°C under unstirred conditions without deaeration. The polarization studies were carried out from a potential of +250 to –250 mV with respect to the steady-state potential at a scan rate of 0.5 mVs^{-1} using CHI Electrochemical Analyzer (Model 604A). The linear Tafel segments of the anodic and cathodic curves were extrapolated to obtain corrosion potential (E_{corr}) and corrosion current densities (I_{corr}). The inhibition efficiency was evaluated from the measured I_{corr} values using the relationship[20];

$$\%IE = \frac{I^0_{corr} - I_{corr}}{I^0_{corr}} \times 100 \quad (2)$$

where I°_{corr} is the corrosion current density without inhibitor and I_{corr} is the corrosion current density with inhibitor.

The polarization resistance (R_p) values were calculated by performing linear polarization experiments in the potential range $E_{corr} \pm$ 10 mV with the scan rate of 0.1 mVs^{-1}. The potential-current characteristic in this range of potential follows the Ohm's law and is termed as linear polarization. The slope of overpotential (η) vs. current density (*i*) curves in the vicinity of corrosion potential yielded the value of R_p. From the measured polarization resistance values, the inhibition efficiency has been calculated using the relationship;

$$\%IE = \frac{R_p - R^0_p}{R_p} \times 100 \quad (3)$$

where, R^0_p and R_p are the polarization resistance in the absence and presence of the inhibitor, respectively.

The impedance measurements were carried out using an ac signal of 5 mV amplitude for the frequency spectrum from 100 KHz to 0.01 Hz. The electrode was kept for 30 min in the solution before starting the impedance measurement. The Nyquist representations of the impedance data were analysed with *Zsimpwin* software (marketed by Princeton Applied Research). The charge transfer resistance (R_{ct}), values were obtained from the diameter of the semicircles of the Nyquist plots. The inhibition efficiency of the inhibitor has been calculated from the

charge transfer resistance values using the following equation[20–23]:

$$\%IE = \frac{R_{ct} - R_{ct}^0}{R_{ct}} \times 100 \quad (4)$$

where, R_{ct}^0 and R_{ct} are the charge transfer resistance in the absence and presence of inhibitor.

The interfacial double layer capacitance (C_{dl}) values were obtained from the frequencies at which the imaginary component of the impedance is maximum ($-Z''_{max}$) in the Nyquist plot using following equation[20];

$$f(-Z''_{max}) = \frac{1}{2\pi C_{dl} R_{ct}} \quad (5)$$

RESULTS AND DISCUSSIONS

Weight loss measurements

The corrosion inhibition of mild steel in 0.5*M* H_2SO_4 solution at 35°C containing various concentrations of the Fen-*g*-PAM was studied by weight loss measurements and the data obtained after 24 h of immersion have been recorded in Table I. The results in the table clearly revealed that grafting of polyacrylamide with fenugreek mucilage increases the inhibition efficiency to 94.2%, which was only 72.5% for PAM at 100 ppm. It is also apparent that the inhibition efficiency has increased from 78–94% as the concentration of Fen-*g*-PAM was increased from 1 to 100 ppm by weight. No further increase in the inhibition efficiency was observed on further increase in the inhibitor concentration and therefore these values are not mentioned in the table. Figure 2 shows the variation of inhibition efficiency for 10 ppm of the inhibitor as a function of immersion time. It is evident from the figure that the inhibition efficiency increases very slowly with increasing immersion time and attains an optimum value of 87% at 72 h. The inhibition efficiency beyond 72 h remains constant.

PAM contains nitrogen, and oxygen atoms in its structure having lone pair of electrons. The compound could be adsorbed by the interaction between the lone pairs of electrons of the oxygen and nitrogen atom present in the polymer moiety and the vacant d-orbital on mild steel. In acidic solution, PAM exists in the protonated form. These protonated species are adsorbed on the cathodic sites of the mild steel and thereby decrease the hydrogen evolution reaction. Grafting of PAM with fenugreek mucilage increases the IE to 94.2% which was only 72.5% for PAM at 100 ppm. This increase in IE may be due to participation of oxygen atom in the aldehydic group of Fen-*g*-PAM and/or its larger surface area. The increase in IE with the concentration of Fen-*g*-PAM is because of the availability of larger number of molecules for adsorption at higher concentrations. No further increase in IE beyond 100 ppm of Fen-*g*-PAM is attributed to the saturation of adsorption process.

TABLE I
Variation of Inhibition Efficiency with Different Concentrations of Fen-*g*-PAM Obtained from Weight Loss Experiments

Concentration (ppm)	Corrosion rate (mg cm^{-2} h^{-1})	Inhibition efficiency (%)
0.0	3.660	–
1.0	0.801	78.1
5.0	0.620	83.0
10	0.573	84.3
20	0.455	87.5
40	0.408	88.8
60	0.361	90.1
80	0.251	93.1
100	0.212	94.2

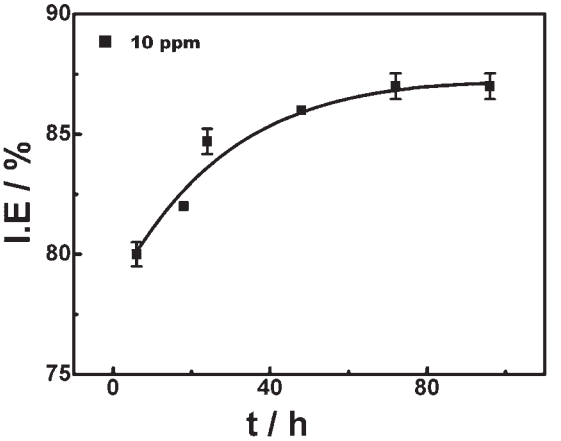

Figure 2 Variation of inhibition efficiency with immersion time of electrode. (%I.E. = Percentage inhibition efficiency, t = immersion time of electrode).

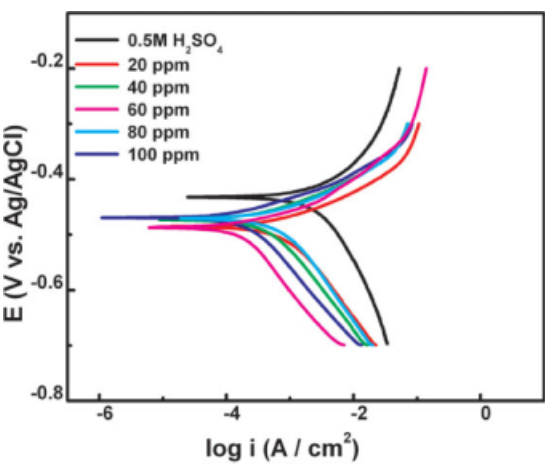

Figure 3 Potentiodynamic polarization behavior of mild steel in 0.5*M* H_2SO_4 with the addition of different concentration of Fen-*g*-PAM at 35°C. [Color figure can be viewed in the online issue, which is available at www.interscience.wiley.com.]

TABLE II
Corrosion Kinetic Parameters of Mild Steel in 0.5*M* H_2SO_4 with Fen-*g*-PAM at 35°C

Concentration (ppm)	E_{corr} (mV vs. Ag/AgCl)	βa (mV/dec)	βc (mV/dec)	I_{corr} (μA/cm^2)	Surface coverage (θ)	I.E (%)
0.0	−432	161	177	4399	–	–
1.0	−473	101	138	931.7	0.788	78.8
5.0	−461	109	147	915.6	0.792	79.2
10	−487	121	158	903.6	0.794	79.4
20	−471	101	160	885.7	0.800	80.0
40	−472	90	143	748.9	0.830	83.0
60	−472	86	85	479.7	0.891	89.1
80	−459	114	113	313.8	0.929	92.9
100	−466	79	144	257.3	0.941	94.1

Potentiodynamic polarization studies

The potentiodynamic polarization behavior of mild steel in 0.5*M* H_2SO_4 with the addition of different concentrations of Fen-*g*-PAM at 35°C is shown in Figure 3. The corrosion parameters viz. corrosion potential E_{corr}, corrosion current density I_{corr}, anodic Tafel slopes (β_a), cathodic Tafel slopes (β_c) derived from these curves are given in Table II. It is noted from the table that corrosion current values (I_{corr}) decrease from 4399 μA cm^{-2} to 257.3 μA cm^{-2} with the addition of 100 ppm of Fen-*g*-PAM. Further, the addition of Fen-*g*-PAM alters the values of E_{corr} toward negative direction and at the same time at each potential the cathodic current decreases with respect to blank (without inhibitor) solution. This indicates that the Fen-*g*-PAM acts as a cathodic inhibitor. The anodic current, however, increases on the addition of inhibitor indicating the acceleration of anodic process. The observed decrease in the I_{corr} is due to larger retardation of cathodic reaction as compared with the corresponding increase in the anodic reaction rate. The anodic and cathodic slope values in the presence of inhibitor are always smaller than those in its absence. However, with change in concentration of inhibitor no particular trend emerges from the data and therefore it is difficult to explain these values.

It has been found from the linear polarization studies (Table III) that the polarization resistance gradually increases with increase in inhibitor concentration. The polarization resistance (R_p) reaches a maximum of 87 Ω cm^2 with the addition of 100 ppm of Fen-*g*-PAM, which is only 7.0 Ω cm^2 for the blank solution. The magnitude of R_p indicates the degree of retardation of H^+ reduction and metal dissolution processes at the interface.

Electrochemical impedance spectroscopy

The impedance behavior of mild steel in 0.5*M* H_2SO_4 with the addition of various concentrations of Fen-*g*-PAM is shown in Figure 4. The charge transfer resistance (R_{ct}) is calculated from the difference in impedance at lower and higher frequencies, as suggested by Haruyama and Tsuru.[22] These curves show a single semicircle indicating the occurrence of single charge transfer reaction. The impedance diagrams are not perfect semicircles[24] instead these curves are depressed in nature with the center below the x- axis. This is because of the presence of micro roughness and other inhomogeneties of the solid electrode formed during the process of corrosion.[24–26]

The impedance parameter R_{ct} obtained from these curves is given in Table III. The charge transfer

TABLE III
Electrochemical Impedance and Linear Polarization Parameters for Mild Steel in 0.5*M* H_2SO_4 with Fen-*g*-PAM

	Impedance method				LPR method	
Concentration (ppm)	R_{ct} (Ω cm^2)	C_{dl} (μF cm^{-2})	I.E (%)	Surface coverage (θ)	R_p (Ω cm^2)	I.E (%)
0.0	4.0	73	–	–	7.0	–
1.0	25.2	69	84.1	0.841	30	76.6
5.0	40.3	53	90.1	0.901	33	78.8
10	48.2	53	91.7	0.917	51	86.3
20	53.8	51	92.6	0.926	53	86.8
40	63.0	50	93.6	0.936	63	88.8
60	69.3	44	94.2	0.942	69	89.8
80	82.5	40	95.1	0.951	72	90.3
100	97.2	35	95.9	0.959	87	91.9

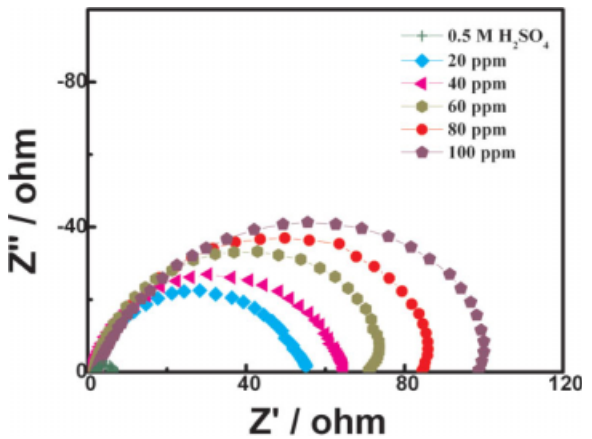

Figure 4 Nyquist plots of mild steel in 0.5*M* H_2SO_4 with the addition of different concentration of Fen-*g*-PAM at 35°C. (Z′ = Real impedance, Z′′ = Imaginary impedance). [Color figure can be viewed in the online issue, which is available at www.interscience.wiley.com.]

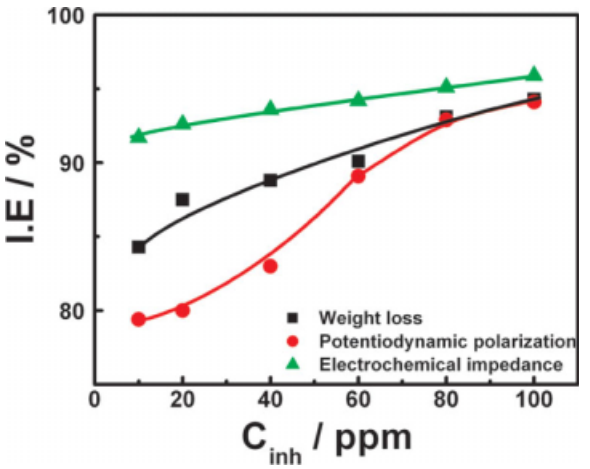

Figure 5 Variation of inhibition efficiency with different concentrations of Fen-*g*-PAM by weight loss and various electrochemical methods. [Color figure can be viewed in the online issue, which is available at www.interscience.wiley.com.]

resistance of blank solution is increased from 4 Ω cm^2 to 97 Ω cm^2 on the addition of 100 ppm of Fen-*g*-PAM resulting in 96% inhibition efficiency. The increase in R_{ct} value is attributed to the formation of a protective film on the metal/solution interface.[27,28] The double layer capacitance (C_{dl}) is decreased from73 μF cm^{-2} to 35 μF cm^{-2} for treatment with 100 ppm of Fen-*g*-PAM. The lowering of C_{dl} values occurred due to a decrease in local dielectric constant and/or an increase in the thickness of the electrical double layer.[29] This indicated that the polymer gets adsorbed at the metal-solution interface and thereby the thickness of the double layer is increased. The variation of inhibition efficiency with concentration of Fen-*g*-PAM obtained by weight loss and electrochemical methods is shown in Figure 5. It is noted from the figure that IE obtained from all the three methods increases with increase in the concentration of the inhibitor however; the deviation in the IE values at lower concentration is much larger than at higher concentrations.

Study of adsorption isotherm

Basic information on the interaction between the inhibitor and the mild steel surface can be provided by the Langmuir adsorption isotherm.[30]

$$\frac{C_{inh}}{\theta} = \frac{1}{K_{ads}} + C_{inh} \tag{6}$$

where K_{ads} is the equilibrium constant of the adsorption process, C_{inh} is the inhibitor concentration. The surface coverage (θ) of different concentration of inhibitor in acidic media has been evaluated from weight loss experiments for various concentrations of inhibitor as shown in Table I, using the equation[31];

$$\theta = \frac{W^0 - W}{W^0} \times 100 \tag{7}$$

The validity of the Langmuir isotherm is confirmed from the linearity of the C_{inh}/θ vs. C_{inh} plot having the slope value close to unity as shown in Figure 6. The deviation from unity is described in terms of surface heterogeneity, particularly when corrosion is occurring simultaneously. This suggests that the adsorption of Fen-*g*-PAM on the mild steel surface obeyed a Langmuir's adsorption isotherm.

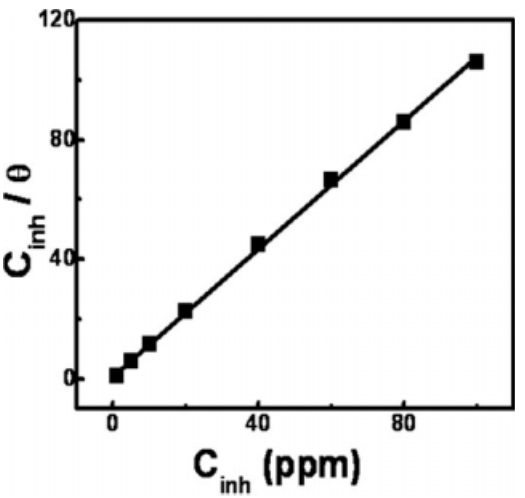

Figure 6 Langmuir adsorption isotherm plot of mild steel in 0.5*M* H_2SO_4 containing different concentrations of Fen-g PAM at 35°C. (C_{inh} = Inhibitor concentration).

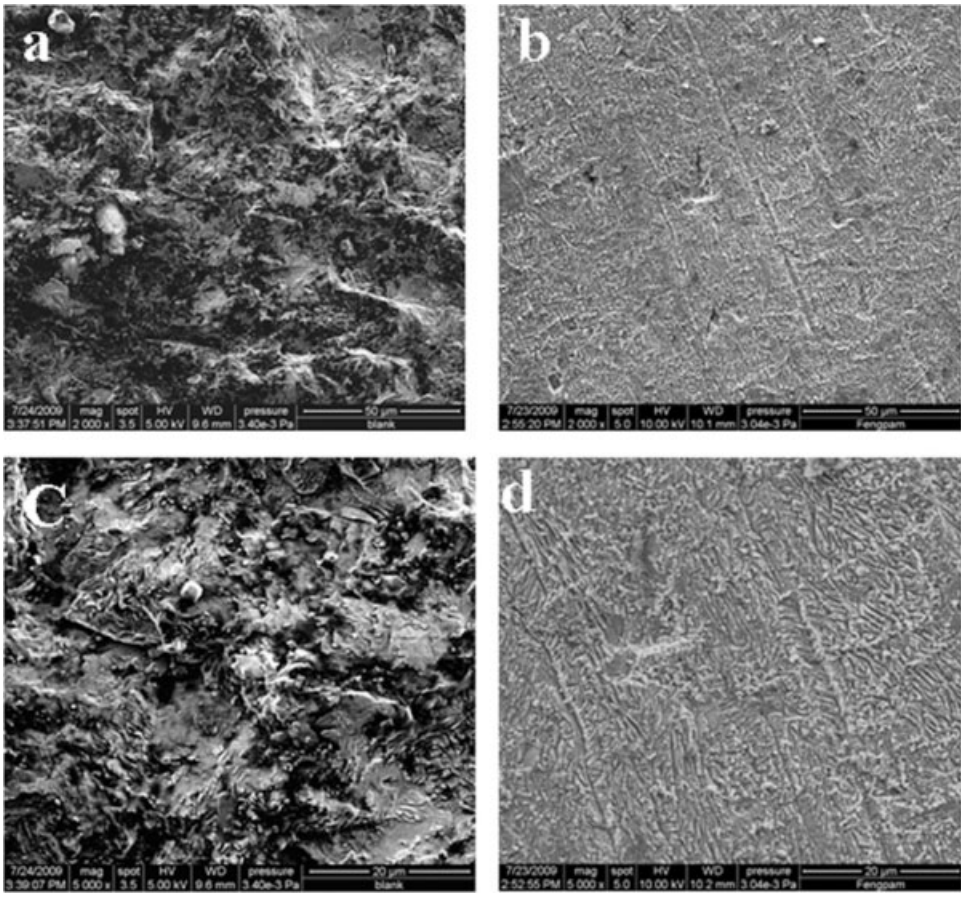

Figure 7 SEM photographs of the surface of mild steel after 24 h of immersion period at 35°C in: (a) 0.5*M* H_2SO_4 at 2000 X (b) 100 ppm of Fen-*g*-PAM at 2000 × 0.5*M* H_2SO_4 at 5000 X (d) 100 ppm of Fen-*g*-PAM at 5000 X.

Surface analysis

SEM photomicrographs for mild steel in 0.5*M* H_2SO_4 solution in the absence and presence of 100 ppm of Fen-*g*-PAM has been depicted in Figure 7(a,b). Figure 7(a) shows a rough surface due to the attack of corrosive medium on the mild steel surface in absence of the inhibitor. On comparing these photomicrographs it appears that in presence of the inhibitor, the surface of the test specimen has improved remarkably with respect to its smoothness. The smoothening of the surface would have been caused

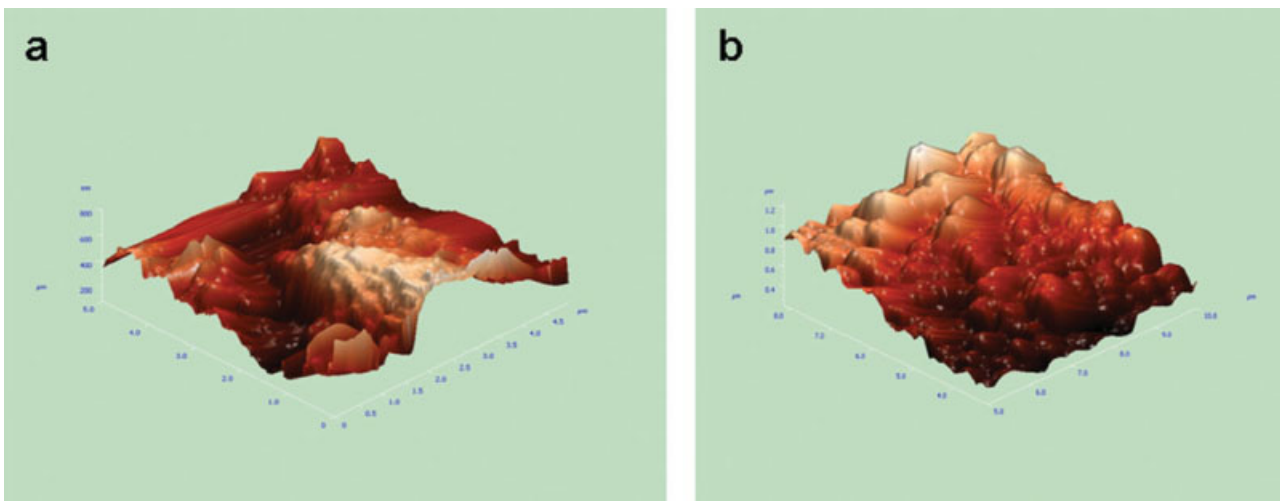

Figure 8 AFM micrographs of mild steel surface (a) 0.5*M* H_2SO_4 (b) 100 ppm of Fen-*g*-PAM. [Color figure can be viewed in the online issue, which is available at www.interscience.wiley.com.]

by the deposition of the Fen-*g*-PAM molecules on steel which protects the surface from the attack of corrosive medium.

Further, surface morphology of the mild steel specimens was studied by Atomic Force Microscopy (AFM) before and after corrosion in presence and absence of Fen-*g*-PAM. The surface morphology supported the formation of adsorbed inhibitor film over the mild steel surface. Figure 8(a) shows the surface morphology (3D) of the mild steel sample corroded in 0.5*M* H_2SO_4 with no inhibitor added to it. The average roughness was calculated as 117 nm. However, in the presence of a 100 ppm of Fen-*g*-PAM retarded the corrosion and surface showed pits and cavities rather than cracks as shown in Figure 8(b). The average surface roughness was calculated as 65 nm, which is probably due to the formation of an inhibitor film over the mild steel surface.

CONCLUSIONS

Polyacrylamide grafted with fenugreek mucilage is an excellent inhibitor for the corrosion of mild steel in 0.5*M* H_2SO_4 and shows an efficiency of 96% at a concentration of 100 ppm. It acts as a cathodic inhibitor in 0.5*M* H_2SO_4, and its inhibition efficiency increases with the inhibitor concentration. The results obtained from weight loss, potentiodynamic polarization, and electrochemical impedance spectroscopy are in reasonably good agreement with each other. Inhibition of corrosion by Fen-*g*-PAM is due to the formation of physically adsorbed Fen-*g*-PAM film on the metal surface. The adsorption of Fen-*g*-PAM on the mild steel surface in 0.5*M* H_2SO_4 obeys a Langmuir adsorption isotherm. The adsorbed film over the mild steel surface has been confirmed by SEM and AFM.

The authors thank P.C. Pandey, Head, Department of Applied Chemistry, IT, BHU for necessary facilities and Dr. Anuradha Mishra, Head, Department of Applied Chemistry, University Institute of Engineering & Technology, C.S.J.M. University, Kanpur for providing the inhibitor.

References

1. Trabanelli, G. Corrosion 1991, 47, 410.
2. Tamilselvi, S.;Raman, V.; Rajendran, N. J Appl Electrochem 2003, 33, 1175.
3. Tebbji, K.; Bouabdellah, I.; Aouniti, A.; Hammouti, B.; Oudda, H.; Benkaddour, M.; Ramdani, A. Mater Lett 2007, 61, 799.
4. Popova, A.; Sokolova, E.; Raicheva, S.; Chritov, M. Corros Sci 2003, 45, 33.
5. Popova, A.; Chritov, M.; Raicheva, S.; Sokolova, E. Corros Sci 2004, 46, 1333.
6. Touhami, F.; Hammouti, B.; Aouniti, A.; Kertit, S. Ann Chim Sci Mat 1999, 24, 581.
7. Schmitt, G. Br Corros J 1984, 19, 165.
8. Bockris, J. O'M.; Yang, B. J Electrochem Soc 1991, 138, 2237.
9. Pillali, C.; Narayan, R. Corros Sci 1983, 23, 151.
10. Bartos, N. J Electrochem Soc 1992, 139, 3429.
11. Ayers, R. C.; Hackerman, N. J Electrochem Soc 1963, 110, 507.
12. Singh, M. M.; Rastogi, R. B.; Upadhyay, B. N. Corrosion 1994, 50, 620.
13. Rastogi, R. B.; Singh, M. M.; Yadav, M. Bull Electrochem 2004, 20, 1.
14. Chetouani, A.; Medjahed, K.; Sid-Lkhdar, K. E.; Hammouti, B.; Mansri, A.; Benaddour, M. Corros Sci 2004, 46, 2421.
15. Jeyaprabha, C.; Sathiyanarayanan, S.; Phani, K. L. N.; Venkatachari, G. J Electroanal Chem 2004, 385, 250.
16. Muller, B. React Funct Polym 1999, 39, 165.
17. Jeyaprabha, C.; Sathiyanarayanan, S.; Phani, K. L. N.; Venkatachari, G. Appl Surf Sci 2005, 252, 966.
18. Grchev, T.; Cvetkovska, M.; Stafilov, T.; Schultze, J. W. Electrochim Acta 1991, 36, 1315.
19. Mishra, A.; Yadav, A.; Pal, S.; Singh, A. 2006, 65, 58.
20. Bentiss, F.; Lagrenee, M.; Traisnel, M.; Hornez, J. C. Corros Sci 1999, 41, 789.
21. Jutter, K. Electrochem Acta 1990, 35, 150.
22. Tsuru, T.; Haruyama, S.; Gijutsu, B. J Jpn Soc Corros Engng 1978, 27, 573.
23. Dus, B.; Szklarska-Smialowska, Z. Corrosion (Nace) 1984, 15, 175.
24. Mansfeld, F.; Kending, M. W.; Tsai, S. Corrosion 1982, 38, 570.
25. Pajkossy, T. J Electroanal Chem 1994, 364, 111.
26. Mansfeld, F. Corrosion 1981, 36, 301.
27. Bentiss, F.; Traisnel, M.; Lagrenee, M. Corros Sci 2000, 42, 127.
28. Murlidharan, S.; Phani, K. L. N.; Pitchumani, S.; Ravichandran, S.; Iyer, S. V. K. J Electrochem Soc 1995, 142, 1478.
29. Mccafferty, E.; Hackermann, N.; Tsai, S. Corrosion 1982, 38, 57.
30. Xu, F.; Duan, J.; Zhang, S.; Hou, B. Mater Lett 2008, 62, 4072.
31. Landolt, D. Corrosion et Chimie de Surface des Metaux, 1st ed.; Alden Press: Oxford, 1993; p 495.